Long-range dielectric confinement

Paul M. Fishbane
Physics Department, University of Virginia, Charlottesville, Virginia 22901

Stephen G. Gasiorowicz
Physics Department, University of Minnesota, Minneapolis, Minnesota 55455

Peter Kaus
Physics Department, University of California, Riverside, California 92521
(Received 18 August 1986; revised manuscript received 2 March 1987)

We discuss the energy of a heavy-quark–antiquark system in a cylindrical and a prolate spheroidal cavity in the dielectric vacuum picture of confinement. We discuss the spin dependence of the energy and compare our results with those of other treatments of quarkonia.

I. INTRODUCTION

A complete analytic or numerical analysis of the long-distance behavior of quantum chromodynamics (QCD) has proven to be elusive, so that the construction of models attempting to represent the important features of QCD continues to be of value. A sufficient number of rather different quarkonium potentials exist[1] to make it clear that the pure phenomenology of quarkonia will never serve as a decisive arbiter for the nonrelativistic potential between quarks, let alone for the behavior of QCD. This is partly because quarkonia exist in the delicate transition region between long distances and short distances, as well as in a region which is neither unambiguously relativistic nor nonrelativistic.

The lattice gauge formalism provides a framework for the numerical calculation of the behavior of QCD. Aside from the fact that numerical results are not as satisfying as analytic ones, progress toward realistic systems such as the observed quarkonia has been frustratingly slow. However, lattice gauge calculations can also serve as a foil or a testing ground for dynamical models whose region of calculability may not be that of observable quarkonia but may precisely be one where the lattice calculations are reliable.

Perhaps the simplest example of this type is the static potential between a very massive (fixed) quark-antiquark pair at large distances. Since all models (and perhaps even QCD itself) lead to potentials which at large distances grow linearly with separation between the sources, what will distinguish different models for the potential are the nonleading terms and the spin structure. One such model,[2] which forms the basis for the calculations performed in this paper, treats the nonlinear aspects of the gluon field and possible effects of light-quark–antiquark pairs through the creation of a cavity in the QCD vacuum. This vacuum has the property that the residual gluon fields, which are treated as Abelian, cannot penetrate it. The vacuum is a region in which the dielectric constant vanishes ($\epsilon=0$) and the magnetic permeability is infinite ($\mu=\infty$), so that the relativistic condition $\epsilon\mu=1$ is maintained. The presence of a sufficiently strong color field leads to a region in which the above QCD vacuum makes a transition to a different phase, with $\epsilon=\mu=1$. We refer to this model as a "dielectric vacuum model" (DVM).

Although this model and the closely related "bags,"[3-5] which in part differ because of the presence of surface tension terms in the energy, have been studied numerically, these studies have been for the most part aimed at phenomenology.[6,3] As mentioned earlier, such studies have not provided conclusive evidence for or against particular models. Our aim is quite different: we want to study the model at large separations and extract analytical results, even at the price of modifying the model in certain ways. Analytic results can give us different insights into the meaning of such a model, and we hope they can be valuable in comparing models with each other and with numerical calculations on the lattice.

When there is a color-singlet quark-antiquark pair with a fixed spacing, the shape of a cavity is determined by the requirement that the electric field $\mathbf{E}$ takes on a constant critical value on the boundary. The behavior of the dielectric constant may change continuously near the boundary, as in the models considered by Adler *et al.*[2] and others,[7] or it may change discontinuously, as treated herein. In the latter case, the electric field must be tangential to the surface. These boundary conditions are identical to those treated numerically in earlier work.[3,8] The resulting cavity will have cusplike singularities near the sources. The complete analytic solution of the analogous problem in two dimensions was determined by Giles[9] with the help of conformal mapping techniques which are unfortunately not applicable to the three-dimensional problem.

The earlier numerical solutions, even though they focused on the small charge separations characteristic of quarkonia, indicated that the long-distance shape of the cavity is either that of a cylinder or at least a long prolate spheroid. Encouraged by these numerical suggestions we have studied the analytic solution for two fixed cavities, an open-ended cylinder on whose axis opposite charges

with magnetic moments are placed and a prolate spheroid with the two charges at the foci. These cavities are not determined self-consistently, but we can check to what degree the constant field boundary conditions are satisfied and therefore to what degree they approach a self-consistent prediction of the DVM.

It is clear that our calculation is nothing more than a simple exercise in electrostatics. However, the results are both transparent and interesting. Even though these cavities represent a mutilation of the exact solution, since they do not have cusplike behavior, the cylinder is close to self-consistent at large separations, and the fact that there are analytic solutions seems to us to be quite useful. In the context of these solutions—in particular for the cylinder—our objective is to study corrections to the expected linear behavior of the potential as well as the behavior of the spin-spin forces.

We find for the cylinder that the nonleading force terms—below the linear and constant terms—fall off exponentially as a function of the parameter $\lambda = a/2R$, where a is the charge separation and R is the cylinder radius. The spin-spin forces also fall off exponentially. Because of the lack of "end caps" and cusplike behavior, we certainly cannot claim that the prediction of our calculation is a prediction of the DVM with sharp dielectric cutoff, but in any case the sharp cutoff case is itself unlikely to be an exact prediction of QCD. The infinite-mass restriction is also not very realistic. For all of these reasons we think direct application to phenomenology of our calculation is unwarranted. Instead, our asymptotic results are meant to stand on their own as a sort of independent model which can be compared with other models or with lattice calculations.

In Sec. II we treat the cylindrical cavity, in the following section we treat the prolate spheroid, and we finish in Sec. IV with some discussion.

II. CYLINDRICAL CAVITY

A. Determination of the potential

We consider a cylinder of radius R, choosing its axis to be the z axis and placing the charges $\pm g$ at $z = \pm a/2$ (see Fig. 1). The potential may be written as the sum of three terms, the potentials ϕ_1 and ϕ_2 due to the charges $\pm g$ and ϕ_h which is a solution of the source-free Laplace equation, and which represents the antiscreening induced charge.

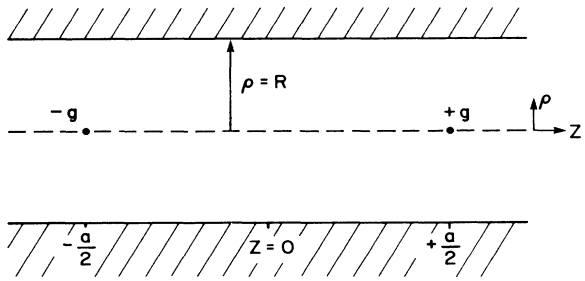

FIG. 1. Two charges on the axis of an uncapped cylinder. Inside, the dielectric constant $\epsilon = 1$, while outside $\epsilon = 0$.

We have [in cylindrical coordinates (ρ,θ,z)]

$$\phi(\mathbf{r}) = \phi_1(\mathbf{r}) + \phi_2(\mathbf{r}) + \phi_h(\mathbf{r}) , \tag{2.1}$$

where

$$\phi_{1,2}(\mathbf{r}) = \pm g \left[\left[z \mp \frac{a}{2} \right]^2 + \rho^2 \right]^{-1/2} . \tag{2.2}$$

Here and throughout the subscript 1 (2) refers to the upper (lower) sign. The homogeneous (background) potential ϕ_h which represents the antiscreening induced charge[3] must satisfy the Laplace equation. Since there is azimuthal symmetry we write

$$\phi_h(\mathbf{r}) = \frac{1}{\pi} \int_{-\infty}^{\infty} dk\, e^{ikz} I_0(k\rho) A(k) . \tag{2.3}$$

This form suggests that $A(k)$ can be determined through the Fourier transform of $\phi_{1,2}$:

$$\phi_{1,2} \equiv \frac{1}{2\pi} \int_{-\infty}^{\infty} dk\, e^{ikz} \tilde{\phi}_{1,2}(k,\rho) , \tag{2.4}$$

determined by

$$\frac{1}{[\rho^2 + (z \pm a/2)^2]^{1/2}} = \frac{1}{\pi} \int_{-\infty}^{\infty} dk\, e^{ik(z \pm a/2)} K_0(|k|\rho) . \tag{2.5}$$

Thus

$$\phi(\mathbf{r}) = \frac{1}{\pi} \int_{-\infty}^{\infty} dk\, e^{ikz} \left[A(k) I_0(k\rho) - 2ig \sin\left[\frac{ka}{2} \right] K_0(|k|\rho) \right] . \tag{2.6}$$

The conditions

$$\left. \frac{\partial \phi}{\partial \rho} \right|_{\rho = R} = 0 \tag{2.7}$$

and $\phi \to_{g \to 0} 0$ imply

$$A(k) = 2ig \sin(\tfrac{1}{2}ka) \frac{d}{d\rho} K_0(|k|\rho) \Big/ \left. \frac{d}{d\rho} I_0(k\rho) \right|_{\rho = R} = -2ig \sin(\tfrac{1}{2}ka) \left[\frac{|k|}{k} \right] K_1(|k|R)/I_1(kR) . \tag{2.8}$$

B. Field characteristics

We begin by checking that the electric flux Φ lies between the charges. We have

$$\Phi(z) \equiv 2\pi \int_0^R \rho\, d\rho \frac{\partial \phi(\rho,z)}{\partial z} . \tag{2.9}$$

Using (2.6) and (2.8), it is easy to check that

$$\Phi(z) = -\frac{2g}{\pi} 2\pi \int_{-\infty}^{\infty} dk \frac{e^{ikz}}{k} \sin\frac{ka}{2} = \begin{cases} 4\pi g, & \frac{a}{2} > z > -\frac{a}{2} , \\ 0, & |z| > \frac{a}{2} . \end{cases} \tag{2.10}$$

For the field at the boundary we evaluate $E_z|_{\rho=R} = -\partial\phi/\partial z|_{\rho=R}$. Dropping terms odd in k from the integral over k, we have

$$E_z\,|_{\rho=R}=\frac{4g}{\pi}\int_0^\infty dk\,k\,\cos kz\,\sin\tfrac{1}{2}ka\left[K_0(kR)+I_0(kR)\frac{K_1(kR)}{I_1(kR)}\right]=\frac{4g}{\pi R}\int_0^\infty dk\,\cos kz\,\sin\frac{ka}{2}\frac{1}{I_1(kR)}\ , \tag{2.11}$$

where we have used the Wronskian of the two Bessel functions. Expanding the product sin× cos in Eq. (2.11) we have

$$E_z\,|_{\rho=R}=\frac{2g}{\pi R^2}\int_0^\infty dx\left[\sin x\frac{z+\frac{a}{2}}{R}-\sin x\frac{z-\frac{a}{2}}{R}\right]\Big/I_1(x)\ . \tag{2.12}$$

For z fixed in the region between the two charges, the behavior of E_z as a function of increasing a is of the form

$$I(\xi)\equiv\int_0^\infty dy\frac{\sin\xi y}{I_1(y)}\quad\text{as }\xi\to\infty\ . \tag{2.13}$$

This function converges very rapidly to π from below; numerical calculation shows that it already lies within 1% of π when ξ rises to 1.5. This is a measure, then, of the constancy of E_z on the boundary between the charges.

We can understand the rapid convergence of $I(\xi)$ with the help of the formula

$$\frac{x}{I_1(x)}=2\sum_{m=1}^{\infty}\frac{\gamma_m{}^2}{J_2(\gamma_m)}\frac{1}{\gamma_m{}^2+x^2}\ ,\qquad J_1(\gamma_m)=0,\quad m=1,2,3,\ldots\ . \tag{2.14}$$

We obtain, for the field,

$$\frac{4g}{R^2}\sum_{m=1}^{\infty}\frac{1}{J_2(\gamma_m)}\times\begin{cases}e^{-\gamma_m z/R}\sinh\gamma_m a/2R, & z>\frac{a}{2}>0\ ,\\ -e^{-\gamma_m a/2R}\cosh\gamma_m z/R+1, & \frac{a}{2}\geq z>0\ .\end{cases} \tag{2.15}$$

Outside of the region between the charges, the field falls off exponentially. In between the charges, aside from exponentially falling terms, the field is given by

$$\frac{4g}{R^2}\sum_{m=1}^{\infty}\frac{1}{J_2(\gamma_m)}=\frac{4g}{R^2}\lim_{x=0}\left[\frac{x}{2I_1(x)}\right]=\frac{4g}{R^2}\ . \tag{2.16}$$

Figure 2 shows the contours of equal boundary field as a function of R for a fixed separation of the charges. These contours suggest the final shape of the self-consistent boundary; in particular we see the cylindrical shape between the charges, as well as the dimple at the exterior axis.

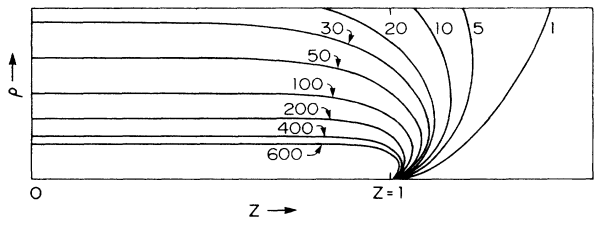

FIG. 2. Field strengths on cylindrical surfaces $\rho=R$. The charges are held at $z=\pm1$, and the surface R is varied to map out the space. For $R\ll a$, much of the field is constant on the surfaces.

C. Calculation of potential

The potential at the charge g can be obtained by calculating

$$U_1=g(\phi_2+\phi_h) \tag{2.17}$$

at $\rho=0$ and $z=a/2$, with the exclusion of the infinite Coulomb self-energy of the charge at $a/2$. We get

$$U_1=-\frac{g^2}{a}+\frac{2ig^2}{\pi}\int_{-\infty}^{\infty}dk\,e^{ika/2}\sin\frac{ka}{2}\frac{k}{|k|}\frac{K_1(|k|R)}{I_1(kR)}$$
$$=-\frac{g^2}{a}+\frac{4g^2}{\pi}\int_0^\infty dk\frac{\sin^2(ka)}{2}\frac{K_1(kR)}{I_1(kR)}\ . \tag{2.18}$$

We need to evaluate the integral

$$S_1(R,a)=\int_0^\infty dk\,\sin^2\frac{ka}{2}\frac{K_1(kR)}{I_1(kR)}\ , \tag{2.19}$$

which may be written in terms of the parameter

$$\lambda=\frac{a}{2R} \tag{2.20}$$

as

$$S_1(R,a)=\frac{1}{R}\int_0^\infty dx\,\sin^2\lambda x\frac{K_1(x)}{I_1(x)}$$
$$\equiv\frac{1}{R}L_1(\lambda)\ . \tag{2.21}$$

The integral $L_1(\lambda)$ is evaluated in the Appendix. It is given by

$$L_1(\lambda)=\frac{\pi}{8\lambda}+\pi\lambda+\pi D+\frac{\pi}{2\lambda}\sum_{m,n}\frac{\gamma_m{}^2\gamma_n{}^2}{J_2(\gamma_m)J_2(\gamma_n)}\frac{1}{\gamma_n{}^2-\gamma_m{}^2}\left[\frac{e^{-2\lambda\gamma_n}}{\gamma_n{}^4}-\frac{e^{-2\lambda\gamma_m}}{\gamma_m{}^4}\right],\quad J_1(\gamma_m)=0,\quad m=1,2,\ldots . \tag{2.22}$$

The constant D is given by

$$D=\sum_{m,n}\frac{\gamma_m{}^2\gamma_n{}^2}{J_2(\gamma_m)J_2(\gamma_n)}\frac{1}{\gamma_n{}^2-\gamma_m{}^2}\left[\frac{1}{\gamma_n{}^3}-\frac{1}{\gamma_m{}^3}\right] \tag{2.23}$$

and it can be evaluated numerically. We find

$$D=-0.552\ . \tag{2.24}$$

The leading term in $L_1(\lambda)$ cancels the Coulomb contribution, and we end up with a linear potential and exponential terms:

$$U_1=\frac{2g^2}{R^2}a+\frac{4g^2}{R}D+\frac{4g^2}{a}\sum_{m,n}\frac{\gamma_m{}^2\gamma_n{}^2/(\gamma_n{}^2-\gamma_m{}^2)}{J_2(\gamma_m)J_2(\gamma_n)}\times\left[\frac{e^{-2\lambda\gamma_n}}{\gamma_n{}^4}-\frac{e^{-2\lambda\gamma_m}}{\gamma_m{}^4}\right]. \tag{2.25}$$

In the limit of a separation of the charges that is small compared with the radius of the cylinder we obtain

$$U_1\simeq-\frac{4g^2}{a}\sum_{m,n}\frac{\gamma_m{}^2\gamma_n{}^2}{J_2(\gamma_m)J_2(\gamma_n)}\frac{\gamma_m{}^2+\gamma_n{}^2}{\gamma_m{}^4\gamma_n{}^4}\ . \tag{2.26}$$

Equation (2.14) yields

$$\sum_{m=1}^{\infty}\frac{1}{J_2(\gamma_m)}=1 \tag{2.27}$$

and, by differentiation with respect to x^2 and setting $x=0$, we see that

$$\sum_{m=1}^{\infty}\frac{1}{\gamma_m{}^2J_2(\gamma_m)}=\frac{1}{8} \tag{2.28}$$

which leads to the expected Coulomb potential $-g^2/a$ in Eq. (2.26). Collecting our results we get, for large separation a,

$$U_1=\frac{4g^2}{R}\left[\frac{a}{2R}+D\right]. \tag{2.29}$$

D. Spin-spin potential

The calculation of the spin-spin interaction follows the standard hyperfine interaction calculation. We assume that due to internal spins $\mathbf{S}_1$ and $\mathbf{S}_2$ the (fixed) charges in the cylinders have magnetic moments $\boldsymbol{\mu}_1$ and $\boldsymbol{\mu}_2$, respectively, and the vacuum (the region external to the cylinder) is characterized by magnetic permeability $\mu=\infty$, while inside $\mu=1$. The boundary conditions is that the magnetic field parallel to the surface vanishes, i.e.,

$$\mathbf{B}\times\mathbf{n}\,|_{\rho=R}=0\ . \tag{2.30}$$

The boundary condition has the tendency to pull the field out, rather than squeeze it in, as for the electric field, so that we expect a weakening of the "bare" dipole-dipole interaction. We shall see that this is indeed the case. For a magnetostatic field we may write

$$\mathbf{B}=-\nabla\psi(\mathbf{r})\ . \tag{2.31}$$

The full potential is

$$\psi(\mathbf{r})=\psi_1(\mathbf{r})+\psi_2(\mathbf{r})+\psi_h(\mathbf{r})\ , \tag{2.32}$$

where ψ_h is, as before, the background field and ψ_i is the field due to dipole i:

$$\begin{aligned}\psi_1(\mathbf{r})&=-\frac{1}{4\pi}\boldsymbol{\mu}_1\cdot\nabla\frac{1}{[\rho^2+(z-a/2)^2]^{1/2}}\\&=-\frac{1}{4\pi}\left[(\mu_{1x}\cos\theta+\mu_{1y}\sin\theta)\frac{\partial}{\partial\rho}+\mu_{1z}\frac{\partial}{\partial z}\right]\frac{1}{[\rho^2+(z-a/2)^2]^{1/2}}\ ,\\\psi_2(\mathbf{r})&=-\frac{1}{4\pi}\left[(\mu_{2x}\cos\theta+\mu_{2y}\sin\theta)\frac{\partial}{\partial\rho}+\mu_{2z}\frac{\partial}{\partial z}\right]\frac{1}{[\rho^2+(z+a/2)^2]^{1/2}}\ .\end{aligned} \tag{2.33}$$

We use Eq. (2.5), and we write $\psi_h(\mathbf{r})$, which is a regular solution of Laplace's equation and is written to reflect the possible azimuthal dependence, as

$$\psi_h(\mathbf{r})=\frac{1}{4\pi^2}\int_{-\infty}^{\infty}dk\,e^{ikz}[C_0(k)I_0(k\rho)+C_1(k)\cos\theta I_1(k\rho)+D_1(k)\sin\theta I_1(k\rho)]\ . \tag{2.34}$$

The boundary conditions read

$$\frac{\partial}{\partial\theta}(\psi_1+\psi_2+\psi_h)_{\rho=R}=0,\quad\frac{\partial}{\partial z}(\psi_1+\psi_2+\psi_h)_{\rho=R}=0\ , \tag{2.35}$$

for all θ and z. A little algebra leads to

$$C_0(k)=+ik(e^{-ika/2}\mu_{1z}+e^{ika/2}\mu_{2z})K_0(|k|R)/I_0(kR)\ , \tag{2.36a}$$

$$C_1(k)=-|k|(e^{-ika/2}\mu_{1x}+e^{ika/2}\mu_{2x})K_1(|k|R)/I_1(kR)\ , \tag{2.36b}$$

$$D_1(k)=-|k|(e^{-ika/2}\mu_{1y}+e^{ika/2}\mu_{2y})K_1(|k|R)/I_1(kR)\ . \tag{2.36c}$$

The energy of interaction at the location of μ_1 is

$$U_{\rm mag}=-\boldsymbol{\mu}_1\cdot[\mathbf{B}(\mathbf{R}_1)-\mathbf{B}_1(\mathbf{R}_1)]=\boldsymbol{\mu}_1\cdot\nabla(\psi_2+\psi_h)\,|_{\mathbf{r}=\mathbf{R}_1}\ . \tag{2.37}$$

The first term is the usual dipole-dipole form:

$$\boldsymbol{\mu}_1\cdot\nabla\psi_2\,|_{\mathbf{r}=\mathbf{R}_1}=-(\boldsymbol{\mu}_1\cdot\boldsymbol{\mu}_2-3\mu_{1z}\mu_{2z})/4\pi a^3\ . \tag{2.38}$$

It is straightforward to compute $\nabla\psi_h$. We find in $[x,y,z]$ coordinates

$$\nabla\psi_h\,|_{\rho=0}=\frac{1}{4\pi^2}\int_{-\infty}^{\infty}dk\,ke^{ikz}[\tfrac{1}{2}C_1,\tfrac{1}{2}D_1,iC_0]\ ;$$

hence

$$\begin{aligned}\boldsymbol{\mu}_1\cdot\nabla\boldsymbol{\psi}_h(\mathbf{R}_1)&=\frac{1}{4\pi^2}\int_{-\infty}^{\infty}dkk\{-\tfrac{1}{2}|k|[(\mu_{1x}{}^2+\mu_{1y}{}^2)+(\mu_{1x}\mu_{2x}+\mu_{1y}\mu_{2y})(\cos ka+i\sin ka)]K_1(|k|R)/I_1(kR)\\&\qquad-k[\mu_{1z}{}^2+\mu_{1z}\mu_{2z}(\cos ka+i\sin ka)]K_0(|k|R)/I_0(kR)\}\\&=\frac{1}{2\pi^3R^3}\int_0^{\infty}dx\,x^2\{-\tfrac{1}{2}[(\mu_{1x}{}^2+\mu_{1y}{}^2)+(\mu_{1x}\mu_{2x}+\mu_{1y}\mu_{2y})\cos 2\lambda x]K_1(x)/I_1(x)\\&\qquad-(\mu_{1z}{}^2+\mu_{1z}\mu_{2z}\cos 2\lambda x)K_0(x)/I_0(x)\}\ ,\end{aligned} \tag{2.39}$$

where we have eliminated terms odd in k.

The "induced" terms involving $\mu_1{}^2$ contribute only an a-independent constant to the energy, and we ignore them. The remaining terms are of the form

$$\begin{aligned}\boldsymbol{\mu}_1\cdot\nabla\psi_h\,|_{\mathbf{r}=\mathbf{R}_1}&=-\frac{1}{4\pi^3R^3}(\mu_{1x}\mu_{2x}+\mu_{1y}\mu_{2y})\int_0^{\infty}dx\,x^2\cos 2\lambda xK_1(x)/I_1(x)\\&\quad-\frac{1}{2\pi^3R^3}\mu_{1z}\mu_{2z}\int_0^{\infty}dx\,x^2\cos 2\lambda xK_0(x)/I_0(x)\ .\end{aligned} \tag{2.40}$$

These integrals are calculated in the Appendix. We are left with exponential terms only:

$$\begin{aligned}U_{\rm mag}\simeq&+\frac{1}{2R^3}(\mu_{1x}\mu_{2x}+\mu_{1y}\mu_{2y})\frac{1}{4\gamma_1^{(0)2}}\left[-\frac{1}{\lambda^2}-\frac{2\gamma_1^{(0)}}{\lambda}-4\gamma_1^{(0)2}\right]e^{-2\lambda\gamma_1^{(0)}}/J_2{}^2(\gamma_1^{(0)})\\&+\frac{1}{R^3}\mu_{1z}\mu_{2z}\frac{1}{4\gamma_0^{(0)2}}\left[-\frac{1}{\lambda^2}-\frac{2\gamma_0^{(0)}}{\lambda}-4\gamma_0^{(0)2}\right]e^{-2\lambda\gamma_0^{(0)}}/J_1{}^2(\gamma_0^{(0)})\ .\end{aligned} \tag{2.41}$$

Since $\gamma_0^{(0)}=2.41$ while $\gamma_1^{(0)}=3.83$, we see that the $\mu_{1z}\mu_{2z}$ term dominates—note this holds even for a $\simeq R$, where $\lambda=\frac{1}{2}$ and it would not make sense to drop the nonleading exponentials. We shall return to the implications of Eq. (2.41) in the next section. It is possible to check, with the help of (A11) and (A16), that for short distances we recover Eq. (2.38), as expected.

III. ELLIPTICAL CAVITY

Figure 3 describes the geometry of a prolate spheroid with charges $\pm g$ at the two foci $\pm a/2$. The appropriate variables (ξ,η,ϕ) are defined by[10]

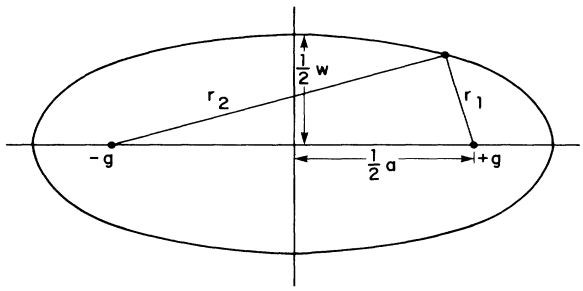

FIG. 3. Two charges at the foci of a prolate spheroid. Inside $\epsilon=1$, while outside $\epsilon=0$.

$$a\xi = r_1 + r_2, \quad a\eta = r_2 - r_1 \ . \tag{3.1}$$

ξ runs from 1 to ∞ and $\xi = 1$ labels the line between the charges. η runs from -1 to 1. The plane midway between the charges perpendicular to the axis is represented by $\eta = 0$. The surface is described by fixed $\xi = \xi_0$, and, as can be seen by Fig. 3,

$$\lambda = \tfrac{1}{2}a(\xi_0 - 1) \ , \tag{3.2}$$

$$w = \tfrac{1}{2}a(\xi_0^2 - 1)^{1/2} \ . \tag{3.3}$$

With these variables in this geometry, Legendre functions are the natural expansion functions. The inhomogeneous terms in the potential are

$$\phi_1 = + \frac{g}{r_1} = \frac{2g}{a}(\xi - \eta)^{-1} = \frac{2g}{a} \sum_{n=0}^{\infty} (2n+1) P_n(\eta) Q_n(\xi) \ , \tag{3.4a}$$

$$\phi_2 = - \frac{g}{r_2} = - \frac{2g}{a}(\xi + \eta)^{-1} = - \frac{2g}{a} \sum_{n=0}^{\infty} (2n+1)(-1)^n P_n(\eta) Q_n(\xi) \ . \tag{3.4b}$$

We describe the homogeneous term in the potential, regular inside the cavity, as

$$\phi_h = \frac{4g}{a} \sum_{n=0}^{\infty} (2n+1)[A_n P_n(\eta) Q_n(\xi) + B_n P_n(\eta) P_n(\xi)] \ . \tag{3.5}$$

Application of the boundary condition $\partial\phi/\partial\xi \mid_{\xi=\xi_0} = 0$ together with $\phi_h \to_{g \to 0} 0$ gives

$$A_n = 0 \quad \text{all } n \ , \tag{3.6a}$$

$$B_n = -Q_n'(\xi_0)/P_n'(\xi_0), \quad n \text{ odd} \tag{3.6b}$$

$$= 0, \quad n \text{ even} \ . \tag{3.6c}$$

We can compute the flux $\Phi(\eta)$ across a given surface η to check that all the flux is contained in the cavity. Given the potential

$$\phi = \frac{4g}{a} \sum_{n \text{ odd}} (2n+1) P_n(\eta) \left[Q_n(\xi) - P_n(\xi) \frac{Q_n'(\xi_0)}{P_n'(\xi_0)} \right] , \tag{3.7}$$

the flux, as a function of η, is given by

$$\Phi(\eta) = 2\pi \frac{a}{2} \int_1^{\xi_0} d\xi (1-\eta^2) \frac{\partial\phi}{\partial\eta} = 4\pi g (1-\eta^2) \sum_{\text{odd}} (2n+1) P_n'(\eta) \int_1^{\xi_0} d\xi [Q_n(\xi) - P_n(\xi) Q_n'(\xi_0)/P_n'(\xi_0)] \ . \tag{3.8}$$

The integrations over ξ can be done in closed form. We find

$$\Phi(\eta) = -4\pi g (1-\eta^2) \sum_{\text{odd}} \frac{2n+1}{n(n+1)} P_n'(\eta) \ ,$$

and, using a standard recursion relation,

$$\Phi(\eta) = 4\pi g \sum_{\text{odd}} [P_{n+1}(\eta) - P_{n-1}(\eta)] \ .$$

In the sum the P's cancel in pairs, leaving only $P^0(\eta) = 1$:

$$\Phi(\eta) = -4\pi g \ . \tag{3.9}$$

The potential ϕ_h at the right-hand charge is given by

$$V \equiv \phi_h \mid_{\eta = 1 = \xi} = - \frac{4g}{a} \sum_{\text{odd}} (2n+1) Q_n'(\xi_0)/P_n'(\xi_0) \ . \tag{3.10}$$

The sum converges rapidly. The denominator is obtained with the help of the representation

$$P_n(z) = F\left[-n, n+1; 1; \frac{1-z}{2} \right] = 1 - \frac{n(n+1)}{2}(1-z) + \frac{(n-1)n(n+1)(n+2)}{16}(1-z)^2 + \cdots \ .$$

This leads to the expression

$$\frac{1}{P_n'(\xi_0)} \simeq \frac{2}{n(n+1)} \left[1 - \frac{(n-1)(n+2)}{8} \epsilon \right] , \tag{3.11}$$

where

$$\epsilon = \xi_0 - 1 = \left[1 + \frac{4w^2}{a^2} \right]^{1/2} - 1 \approx \frac{2w^2}{a^2} = \frac{1}{2\beta^2} \ll 1 \ . \tag{3.12}$$

β is as in Eq. (2.19), with R replaced by w. Using

$$Q_n(\xi_0) = \int_{-1}^{1} dx \frac{P_n(x)}{\xi_0 - x}$$

and

$$\sum_{n=1}^{\infty} \left[\frac{1}{n} + \frac{1}{n+1} \right] P_n(x) = -1 - \frac{\ln(1-x)}{2} \ ,$$

$$\sum_{n=1}^{\infty} (2n+1) P_n(x) = [2(1-x)]^{-1/2} \ ,$$

we end up with

$$V=-\frac{4g}{a}\frac{\partial}{\partial\epsilon}\int_{-1}^{1}dx\left[\frac{1}{1-x+\epsilon}-\frac{1}{1+x+\epsilon}\right]\left[\left[1+\frac{\epsilon}{2}\right]\ln\frac{1-x}{2}+\frac{\epsilon}{4\sqrt{2}}(1-x)^{-1/2}\right]$$
$$=-\frac{4g}{a}\frac{\partial}{\partial\epsilon}\int_{0}^{1}2\,du\left[\frac{1}{2u+\epsilon}-\frac{1}{2-2u-\epsilon}\right]\left[\left[1+\frac{\epsilon}{2}\right]\ln u+\frac{\epsilon}{8\sqrt{u}}\right]. \tag{3.13}$$

The dominant contributions for $\epsilon \ll 1$ are

$$-\frac{4g}{a}\frac{\partial}{\partial\epsilon}\left[-\frac{1}{2}\left[\ln\frac{\epsilon}{2}\right]^2+\frac{\pi}{4\sqrt{2}}\sqrt{\epsilon}\right]. \tag{3.14}$$

Upon differentiation we find

$$V=-\left[\frac{8g}{w}\beta\ln\beta+\frac{8g}{w}\beta\ln 2\right]+\frac{g\pi}{4w}. \tag{3.15}$$

High-order terms in (3.11) contribute further to the term linear in β. A numerical fit of the form of Eq. (3.16) gives a best fit

$$\phi_h \mid_{\eta=1=\xi}=+2\frac{g}{w}(4.04\beta\ln\beta+1.93\beta+1.05). \tag{3.16}$$

The width of the cavity could vary with a, but there is no choice of variation that brings this into a linear form. The logarithmic enhancement is associated with the fact that the prolate spheroid squeezes in close to the charges as $a\rightarrow\infty$.

We can see this by computing the field at the boundary

$$E_{\|}\mid_{\xi=\xi_0}=-\nabla_\eta\phi\mid_{\xi=\xi_0}$$
$$=-\frac{2}{a}(1-\eta^2)^{1/2}(\xi_0^2-\eta^2)^{1/2}\left[\frac{\partial\phi}{\partial\eta}\right]\Bigg|_{\xi=\xi_0}. \tag{3.17}$$

Using our expressions for ϕ and the Wronskian of P_n and Q_n, we find

$$E_\eta\mid_{\xi=\xi_0}=-\frac{4g}{a^2}(\xi_0^2-1)^{-1}(1-\eta^2)^{1/2}(\xi_0^2-\eta^2)^{-1/2}$$
$$\times\sum_{n\ \text{odd}}(2n+1)P_n'(\eta)/P_n'(\xi_0). \tag{3.18}$$

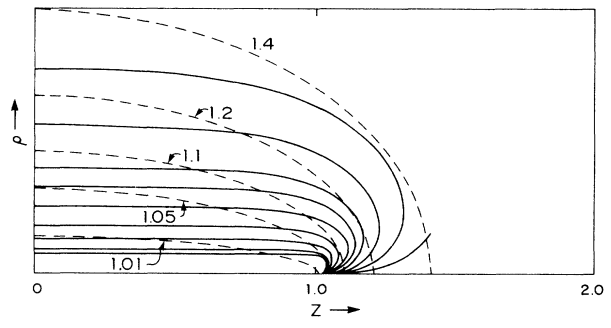

FIG. 4. Field strengths on prolate spheroidal surfaces. Also shown (dashed lines) are the shapes of various spheroids with ξ_0 indicated. The separation of the charges (at the foci) is held fixed and the eccentricity changes. The boundary field is not approximately constant on the surfaces.

A calculation similar to that outlined for the potential yields

$$E_\eta=-\frac{4g}{w}\beta\left[\frac{1}{(1-\eta^2)[(1+2\epsilon)^2-\eta^2]}\right]^{1/2} \tag{3.19}$$

for the leading term. In contrast with the field on the boundary of the cylinder, the field varies quite significantly with η, and becomes very strong as $\eta\rightarrow\pm1$. There nonleading terms become very important. A numerical calculation of the field is shown in Fig. 4, where contours of equal boundary field are plotted, with the configuration so scaled that the charges always appear at fixed $\pm1(a=2)$. Increasing the charge separation translates into narrower prolate spheroids. The figure also shows prolate spheroids of various ξ.

IV. COMMENTS

We begin with a few comments on phenomenology. The open cylinder geometry, as obviously unrealistic as it is, has some properties which are not too far from what we know of physical quarkonia or of lattice calculations of QCD. In order to gain some insight into the values of the two parameters, the charge g and the cylinder radius R, we can compare the potential (2.29) with standard phenomenological potentials[1,11] of the form

$$V(a)=\kappa a-\frac{\alpha}{a}+V_0. \tag{4.1}$$

Since the DVM potential as we have calculated it is never a sum of Coulomb and linear terms, we compare (4.1) separately with the long-range form (2.29) and the short-range Coulomb form, the first term of Eq. (2.18). We have, from Eqs. (2.18), (2.29), and (2.24),

$$\alpha=g^2,\quad \kappa=2g^2/R^2,$$

and

$$V_0=(4g^2/R)\pi D=-(0.552)(4g^2/R^2).$$

We now take the phenomenological values from physical quarkonium,

$$0.3<\alpha<0.5,\quad 0.15<\kappa<0.25\ \text{GeV}^2,$$

implying a range for R and hence for V_0:

$$0.3<R<0.5\ \text{fm},\quad -0.7<V_0<-0.3\ \text{GeV}.$$

In turn, the exponential terms which mark the passage from the Coulomb to the flux-tube regime will have a range $\rho=R/\gamma_1^{(0)}$:

$$0.08<\rho<0.13,$$

in fair accordance with other estimates.[12]

These parameters are at the same time a warning that any detailed comparison of the analytic results of the open cylinder geometry must be taken with several grains of salt when they are compared with phenomenology. We have seen that the range of R is not far from the range of separation of the quark-antiquark pair in real quarkonia, several tenths of fermis. But R comparable to a is precisely a range where the open cylinder, without end caps and cusps, would seem particularly inappropriate. Whether the fact that the values of parameters which we find are reasonable follow from a rapid exponential behavior or from pure coincidence we leave as an open question.

The constant V_0 in the DVM is of the correct phenomenological sign, but is about one-half the right size. Phenomenology demands a Coulomb term for $a > 0.2$ fm not present in our model. But the classical model studied in this paper does not include quantum effects such as transverse zero-point oscillations of the flux tube. These supply a Coulomb term (and other inverse powers), the so-called Lüscher term,[13] with an effective coefficient α_L of magnitude $\pi/12 \simeq 0.26$ which sets in when the flux-tube regime begins.[12]

The usual phenomenological quarkonium potentials are written in a form which derives from nonrelativistic reductions[14] of one-particle-exchange (vector and scalar) graphs, and they are treated as potentials that test particles, whatever their charge, respond to. As already indicated at the end of Sec. II E, our basic point of view is that the potential is a property of the two-body system. This means that we cannot think of a potential in which a charge moves, leading to the usual spin-orbit potential. We would have to study a rotating cavity to arrive at a proper description of the spin-orbit forces. We expect that our results will confirm to those described by Buchmüller.[15] Only the kinematical Thomas precession contribution will appear in the DVM model, and this corresponds to a "scalar potential" in the usual description. As noted in Refs. 10 and 11, purely Thomas-type spin-orbit terms associated with the conventional long-range potential are *favored* by conventional phenomenology.

The Thomas spin-orbit terms are distinguished from the dynamical spin-orbit terms (absent in the DVM) in that they are "self"-correlations, i.e., proportional to $\mathbf{s}_1\cdot\mathbf{L}_1$ and $\mathbf{s}_2\cdot\mathbf{L}_2$, rather than of the form $\mathbf{s}_1\cdot\mathbf{L}_2$ and $\mathbf{s}_2\cdot\mathbf{L}_1$ as for the dynamical terms. In a recent paper, Michael[16] tested the question of long-range spin-orbit terms in SU(2) QCD on the lattice. He finds evidence that only the Thomas-type terms are present at long distances.

Using lattice calculations as a guide to whether a particular model of QCD is sensible seems to us to be a useful approach. In particular, it would be interesting to see whether the spin-spin forces as described here make sense, in particular the a-independent "self"-correlations and the rapidly falling $(\mathbf{s}_1\cdot\mathbf{s}_2)$-type terms as in Eq. (2.36).

APPENDIX

We outline in detail some of the calculations leading to the form of the potential for the cylindrical cavity. Let us first consider the integral

$$S_1(R,a)=\int_0^\infty dk\,\sin^2\frac{ka}{2}\,\frac{K_1(kR)}{I_1(kR)}=\frac{1}{R}L_1(\lambda)\ , \tag{A1}$$

where

$$L_1(\lambda)=\int_0^\infty dx\,\sin^2\lambda x\,\frac{K_1(x)}{I_1(x)}\ . \tag{A2}$$

Now

$$\frac{\partial}{\partial R}S_1(R,a)\bigg|_{a\ \text{fixed}}=\int_0^\infty dk\,\sin^2\frac{ka}{2}\,k\left[\frac{K_1'(kR)}{I_1(kR)}-\frac{K_1(kR)I_1'(kR)}{[I_1(kR)]^2}\right]=-\frac{1}{R^2}\int_0^\infty dx\,\sin^2\lambda x\,\frac{1}{[I_1(x)]^2}\ .$$

The left-hand side has the form

$$\left[\frac{\partial}{\partial R}+\frac{\partial\lambda}{\partial R}\frac{\partial}{\partial\lambda}\right]\frac{1}{R}L_1(\lambda)=-\frac{1}{R^2}L_1-\frac{a}{2R^2}\frac{1}{R}\frac{dL_1}{d\lambda}=-\frac{1}{R^2}\left[L_1+\lambda\frac{dL_1}{d\lambda}\right]\ . \tag{A3}$$

Thus

$$\frac{d}{d\lambda}[\lambda L_1(\lambda)]=\int_0^\infty dx\,\sin^2\lambda x\,\frac{1}{[I_1(x)]^2}\ . \tag{A4}$$

Using

$$\frac{x}{I_1(x)}=2\sum_m\frac{\gamma_m^2}{J_2(\gamma_m)}\frac{1}{\gamma_m^2+x^2} \tag{A5}$$

we get

$$\begin{aligned}\frac{d}{d\lambda}[\lambda L_1(\lambda)]&=4\sum_{mn}\frac{\gamma_m^2\gamma_n^2}{J_2(\gamma_m)J_2(\gamma_n)}\int_0^\infty dx\,\sin^2\lambda x\left[\frac{1}{\gamma_n^2-\gamma_m^2}\left[\frac{1}{\gamma_n^2}\frac{1}{\gamma_n^2+x^2}-\frac{1}{\gamma_m^2}\frac{1}{\gamma_m^2+x^2}\right]+\frac{1}{\gamma_m^2\gamma_n^2x^2}\right]\\&=4\sum_{mn}\frac{\pi\lambda/2}{J_2(\gamma_m)J_2(\gamma_n)}+4\sum_{mn}\frac{\gamma_m^2\gamma_n^2}{J_2(\gamma_m)J_2(\gamma_n)}\frac{\pi}{4}\frac{1}{\gamma_n^2-\gamma_m^2}\left[\frac{1-e^{-2\lambda\gamma_n}}{\gamma_n^3}-\frac{1-e^{-2\lambda\gamma_m}}{\gamma_m^3}\right]\ .\end{aligned} \tag{A6}$$

Setting $x=0$ in (A5) yields

$$\sum_m \frac{1}{J_2(\gamma_m)}=1 \tag{A7}$$

so that

$$\frac{d}{d\lambda}[\lambda L_1(\lambda)]=2\pi\lambda+\pi\sum_{mn}\frac{\gamma_m{}^2\gamma_n{}^2}{J_2(\gamma_m)J_2(\gamma_n)}\frac{1}{\gamma_n{}^2-\gamma_m{}^2}\left[\frac{1-e^{-2\lambda\gamma_n}}{\gamma_n{}^3}-\frac{1-e^{-2\lambda\gamma_m}}{\gamma_m{}^3}\right]. \tag{A8}$$

Hence

$$\lambda L_1(\lambda)=C+\pi\lambda^2+\pi\lambda\sum_{mn}\frac{\gamma_m{}^2\gamma_n{}^2}{J_2(\gamma_m)J_2(\gamma_n)}\frac{1}{\gamma_n{}^2-\gamma_m{}^2}\left[\frac{1}{\gamma_n{}^3}-\frac{1}{\gamma_m{}^3}\right]$$
$$+\frac{\pi}{2}\sum_{m,n}\frac{\gamma_m{}^2\gamma_n{}^2}{J_2(\gamma_m)J_2(\gamma_n)}\frac{1}{\gamma_n{}^2-\gamma_m{}^2}\left[\frac{e^{-2\lambda\gamma_n}}{\gamma_n{}^4}-\frac{e^{-2\lambda\gamma_m}}{\gamma_m{}^4}\right]. \tag{A9}$$

The constant may be evaluated by considering the limit $\lambda=0$. We get

$$C=-\frac{\pi}{2}\sum_{m,n}\frac{\gamma_m{}^2\gamma_n{}^2}{J_2(\gamma_m)J_2(\gamma_n)}\frac{1}{\gamma_n{}^2-\gamma_m{}^2}\frac{\gamma_m{}^4-\gamma_n{}^4}{\gamma_m{}^4\gamma_n{}^4}=\pi\sum_m\frac{1}{J_2(\gamma_m)}\sum_n\frac{1}{\gamma_n{}^2J_2(\gamma_n)}. \tag{A10}$$

Equation (A5) may also be used to obtain

$$\sum_n\frac{1}{\gamma_n{}^2J_2(\gamma_n)}=\frac{1}{8} \tag{A11}$$

so that

$$C=\frac{\pi}{8}$$

and thus

$$L_1(\lambda)=\frac{\pi}{8\lambda}+\pi\lambda+\pi\sum_{mn}\frac{\gamma_m{}^2\gamma_n{}^2}{J_2(\gamma_m)J_2(\gamma_n)}\frac{1}{\gamma_n{}^2-\gamma_m{}^2}\left[\frac{1}{\gamma_n{}^3}-\frac{1}{\gamma_m{}^3}\right]$$
$$+\frac{\pi}{2\lambda}\sum_{mn}\frac{\gamma_m{}^2\gamma_n{}^2}{J_2(\gamma_m)J_2(\gamma_n)}\frac{1}{\gamma_n{}^2-\gamma_m{}^2}\left[\frac{e^{-2\lambda\gamma_n}}{\gamma_n{}^4}-\frac{e^{-2\lambda\gamma_m}}{\gamma_m{}^4}\right]. \tag{A12}$$

The integral needed for the spin-spin potential is

$$\int_0^\infty dk\,k^2\cos ka\frac{K_1(kR)}{I_1(kR)}=\frac{1}{R^3}\int_0^\infty dx\,x^2\cos 2\lambda x\frac{K_1(x)}{I_1(x)} \tag{A13}$$

and this can be obtained from $L_1(\lambda)$, since

$$\int_0^\infty dx\,x^2\cos 2\lambda x\frac{K_1(x)}{I_1(x)}=\frac{1}{2}\frac{d^2}{d\lambda^2}\int_0^\infty dx\sin^2\lambda x\frac{K_1(x)}{I_1(x)}. \tag{A14}$$

The same procedure applies to the evaluation of the other integral in the spin-spin potential,

$$\int_0^\infty dk\,k^2\cos ka\frac{K_0(kR)}{I_0(kR)}, \tag{A15}$$

except that there we use

$$\frac{1}{I_0(x)}=2\sum_m\frac{\eta_m}{J_1(\eta_m)}\frac{1}{\eta_m{}^2+x^2}, \tag{A16}$$

and in the evaluation of the integration constant, we use the result

$$\sum_m\frac{1}{\eta_mJ_1(\eta_m)}=\frac{1}{2} \tag{A17}$$

which follows from (A16).

ACKNOWLEDGMENTS

We thank in particular S. Adler for useful conversations, and the Aspen Center for Physics for its hospitality. P.M.F. was supported in part by the U.S. Department of Energy under Grant No. DE-FG05-84ER40157 and S.G.G. by the U.S. Department of Energy under Grant No. DE-AC02-83ER-40105.

[1]E. Eichten *et al.*, Phys. Rev. D **17**, 3090 (1979); **21**, 203 (1980); J. Richardson, Phys. Lett. **82B**, 272 (1979); W. Buchmüller and S.-H. H. Tye, Phys. Rev. D **24**, 132 (1981); E. Eichten, in *The Sixth Quark,* proceedings of the Twelfth SLAC Summer Institute on Particle Physics, Stanford, 1984, edited by P. M. McDonough (SLAC Report No. 281, SLAC, Stanford, CA, 1985), and references therein; D. Beavis, S.-Y. Chu, B. R. Desai, and P. Kaus, Phys. Rev. D **20**, 2345 (1979); S. Schmitz, D. Beavis, and P. Kaus, this issue, *ibid.* **36**, 184 (1987).

[2]S. Adler, Phys. Rev. D **23**, 2905 (1981); S. Adler and T. Piran, Phys. Lett. **113B**, 405 (1982), **117B**, 91 (1982); Rev. Mod. Phys. **56**, 1 (1984).

[3]P. Gnädig *et al.*, Phys. Lett. **64B**, 62 (1976); P. Hasenfratz *et al.*, *ibid.* **95B**, 299 (1980).

[4]See, e.g., D. Gromes, in *The Quark Structure of Matter,* proceedings of the Yukon Advanced Study Institute, Whitehorse, Yukon, Canada, 1984, edited by N. Isgur, G. Karl, and P. J. O'Donnell (World Scientific, Singapore, 1985).

[5]See, e.g., P. Hasenfratz and J. Kuti, Phys. Rep. **40C**, 75 (1978).

[6]J. R. Hiller, Ann. Phys. (N.Y.) **144**, 58 (1982); Phys. Rev. D **30**, 1520 (1984).

[7]H. Lehmann and T. Wu, Nucl. Phys. **B237**, 205 (1984).

[8]W. Haxton and L. Heller, Phys. Rev. D **22**, 1198 (1980).

[9]R. Giles, Phys. Rev. D **18**, 513 (1978).

[10]See, e.g., P. Morse and H. Feshbach, *Methods of Theoretical Physics* (McGraw-Hill, New York, 1953).

[11]See, e.g., D. Beavis *et al.*, Phys. Rev. D **20**, 2345 (1979).

[12]P. Fishbane, P. Kaus, and S. Meshkov, Phys. Rev. D **33**, 852 (1986).

[13]M. Lüscher, K. Symanzik, and P. Weisz, Nucl. Phys. **B173**, 365 (1980).

[14]D. Gromes, Z. Phys. C **26**, 401 (1984).

[15]W. Buchmüller, Phys. Lett. **112B**, 479 (1982).

[16]C. Michael, Phys. Rev. Lett. **56**, 1219 (1986).